DOI: https://doi.org/10.14311/TPFM.2025.009

EXAMPLE OF REPEATABILITY ISSUE IN A WIND TUNNEL EXPERIMENT MEASURED BY PIV

D. Duda [1], V. Yanovych [1,2], V. Uruba [1,2]

[1] **Faculty of Mechanical Engineering, University of West Bohemia in Pilsen, Univerzitní 22, 306 14 Pilsen, Czech Republic**

[2] **Institute of Thermomechanics of the Czech Academy of Sciences, Dolejškova 5, 180 00 Prague, Czech Republic**

Abstract

A fluid dynamic experiment in a wind tunnel has been repeated in few months. There were used the same equipment (PIV cameras, wind tunnel, model obstacle). The only difference is the time and the assembly. Thus the objective differences are calibration (tried to be as similar as possible) and atmospheric conditions represented by viscosity affecting Reynolds number. In this contribution we show the comparison of these experiments and we discuss the sources of errors decreasing the repeatability. The results are qualitatively same, reproducing even a small symmetry breaking, but they are not exactly the same in a quantitative manner.

Keywords: Repeatability, Reproducibility, Particle Image Velocimetry, Wind tunnel, Vortex.

1 Introduction

Repeatability is a key feature of any scientific experiment and it is a prefactor of *reproducibility* [1]. Reproducibility of an experimental results in different laboratory and at different time, when all important variables are under control and when thus the stated results depend only on those parameters with relevant statistical confidence, is key feature of the scientific seeing of the universe; i.e. that the natural laws does not change in time and space. This assumption allows us to formulate the *approximations* of these transcendent natural laws and later to use their knowledge to predict an experimental result, or to prepare such conditions, which lead to desired results, which is the basis of all technology and therefore of entire modern technical civilization. Thus, reproducibility has principal importance – if some results are not reproducible, it means that (i) there was an error (in original or repeating experiment), or (ii) there was a relevant parameter, which has not been taken into account and thus has not been set to similar value during the repeating experiment.

In an ideal world, every scientific result might be reproduced before publishing ensuring, that the stated conclusions are true and that there is not missing parameter[1]. However, the practice is, that the reviewer usually does not reproduce the experiment, she or he just checks, if the experimental conditions are clearly described in a such way, that the reproduction might be possible in principle (unfortunately, sometimes the important parameters, e.g. geometry, are not presented and such results are published anyway. . .). She or he checks, if results are clearly presented, if the applied analysis makes sense, or if the text is grammatically correct.

In the fluid dynamic experiments, it is proven, that the important parameters are the geometry and the Reynolds number [2], which represents the ratio of important scales of the flow problem. Vincenc Strouhal [3] introduced the time-scale of the fluid response to conditions independent on time. If the frequency plays role among the control parameters, then the Keulegan-Carpenter number [4] is used instead. Oscillating boundary conditions can cause interesting effects even in the problem of heat transfer: Urban et al. [5] has shown, that heat can be pumped in one direction even in the case of zero mean temperature difference just if it oscillates. The Urban number is not yet defined, but it shall be soon. Skrbek et al. [6] has shown, that the accuracy of physical properties of working fluid (especially near the critical point) can have a crucial impact on reproducibility among different laboratories and can easily lead to a false flow regime distinguishing in the case of Rayleigh-Bénard convection.

[1]that would not eliminate all missing parameter: e.g. imagine dependence on gravity acceleration g, which was forgotten in the analysis. Dependence on this parameter would lead to reproducibility fail only in laboratory on different celestial body.

Duda et al. has studied the problem of geometry uncertainty caused by imperfect manufacturing. In article [7] we observed the wake past an airfoil produced at 3 levels of 3D print optimization and we stated, that the largest difference lies near the transition to turbulence, where the slightly different geometry can switch the flow regime. By using hot-wire method [8], finer differences in the turbulence topology were detected. The effect on properties of individual vortices has been shown at this conference in [9].

In this contribution, we performed the same experiment separated in time by 2.5 months. The geometry was the same (physically the same model), the wind tunnel and the measurement equipment were the same as well. Only the date of measurement was separated by 2.5 months. Therefore, the only difference is expected in fluid properties and/or in the repeatability of sample placement and calibration. The fluid state parameters as temperature, pressure and humidity affect Reynolds number via kinematic viscosity, however, those changes are small under typical laboratory conditions.

2 Experimental setup

The experiment is the same as in our previous study [10]: stereo Particle Image Velocimetry (PIV) [11] is used to observe the plane perpendicular to the flow at the outlet of the wind tunnel test section [12]. Inside the wind tunnel test section, there is a *swirler grid* of mesh parameter $M = 25\,\mathrm{mm}$. The strength of the gird is represented via its Rossby number $\mathrm{Ro} = 4/3$, [13]. This grid is located in the distance $z = 500\,\mathrm{mm} = 20 \cdot M$ upstream the measured plane. The wind tunnel velocity is controlled via PID backloop [14] by using measured pressure drop along the contraction section of the wind tunnel. Additionally, the PID regulator measures atmospheric conditions: pressure, temperature and humidity in order to correctly calculate the density and therefore the velocity from measured pressure drop. The directly controlled parameter is the rotational speed of the fan engine, details can be found in [12].

3 Similarities and differences in the results

The results are similar, but *not the same*, see Fig. 1.

First observable difference lies in the Field of View (FoV), which we tried to locate in the same position, however it was not possible exactly and, therefore, even the scale of single grid point is different between compared datasets. The horizontal distance between grid points in the August data is $\Delta_{\mathrm{Aug}} = 2.27\,\mathrm{mm}$, while in October it was $\Delta_{\mathrm{Oct}} = 2.25\,\mathrm{mm}$, i.e. relative error is $8.9 \cdot 10^{-3}$.

The mean velocity (Fig. 1a-c) display vortex lattice in the arrangement as suggested by the grid. The in-plane velocities are displayed by using arrows; the stream-wise velocity w is represented by colour. The vortex centres contain slower fluid, while the inter-vortex areas, we will call them *jets* in this text, are faster. The entire velocity is larger than wind tunnel velocity U due to the growing boundary layers at the tunnel walls, which effectively shrink the cross-section leading to fluid acceleration along the stream. The main discrepancy from lattice regularity is the ellipsoidal shape of the vortices and the consecutive existence of two types of jets: the stronger ones, where the shorten vortex semi-axes meet, and the weaker ones, where the longer semi-axes meet. This discrepancy is reproducible, although its level seem to rise during time.

The spatial distribution of turbulent kinetic energy

$$T_{\mathrm{KE}} = \frac{1}{2}\left(\sigma^2[u] + \sigma^2[v] + \sigma^2[w]\right), \tag{1}$$

where σ is the standard deviation calculated as

$$\sigma[u] = \sqrt{\left\langle (u - \langle u \rangle)^2 \right\rangle}, \tag{2}$$

shows dominating signal at the vortex centres caused by the vortex meandering. In article [10] we have shown, that when corrected to the moving vortex, the value of T_{KE} across the vortex remains constant same as in the background. Note that other authors, e.g. [21], observed zero T_{KE}

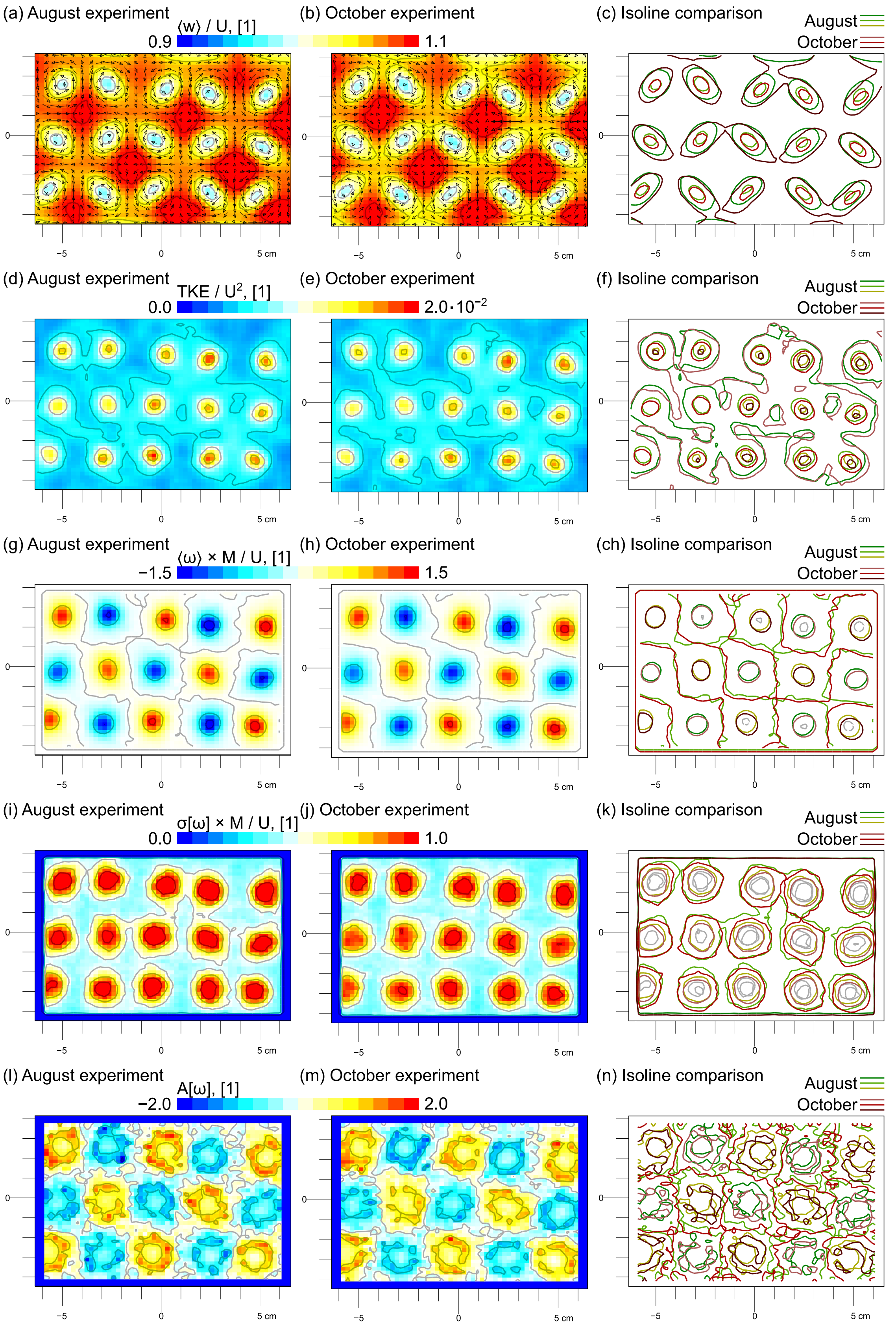

Figure 1: Comparison of the data measured in different moths – left: August experiment, middle: the same experiment repeated 2 months later in October. Right: comparison of isolines of both datasets. Top (a-c): mean stream-wise velocity $\langle w \rangle$ normalized by wind tunnel velocity U. Second (d-f): turbulent kinetic energy; third (g-ch): mean stream-wise vorticity; fourth (i-k): standard deviation of such vorticity and bottom (l-n): skewness (or third statistical moment) of vorticity, $A[\omega] = \left\langle (\omega - \langle \omega \rangle)^3 \right\rangle / \sigma^3[\omega]$.

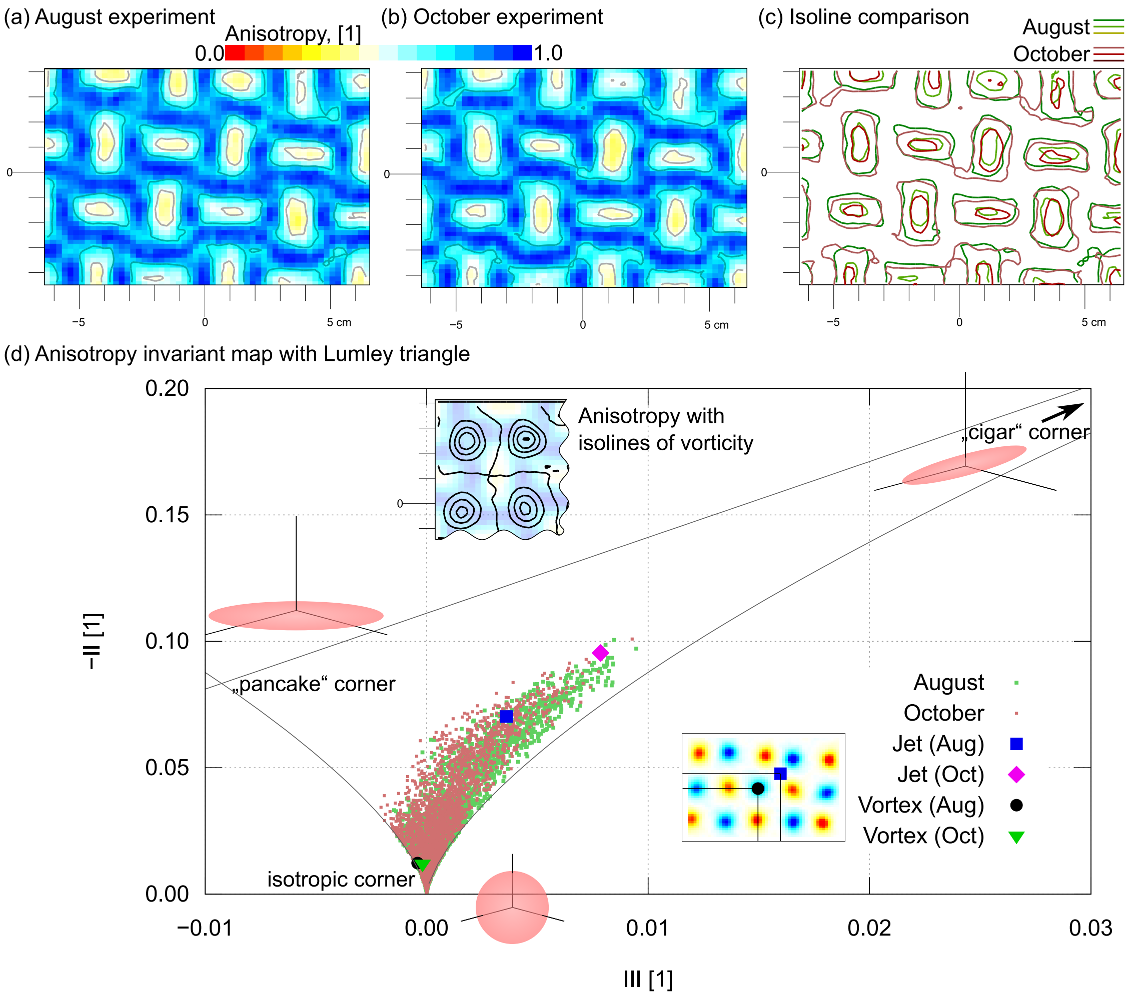

Figure 2: Lumley's anisotropy coefficient [15] $F = 1 + 27 \cdot \mathrm{III} + 9 \cdot \mathrm{II}$, where II and III are the second and third invariant of the Reynolds stress tensor calculated by using Cayley-Hamilton theorem [16, 17]. For fully isotropic distribution of fluctuations, $F = 0$, while for anisotropic $F = 1$. The areas of equilibrium vortex positions contain a *cross* of the anisotropy signal and, surprisingly, it does not have maximum directly in the vortex centre, the maxima are on the lines between neighbouring vortices, but these lines are advected by the circumferential vortex velocity. This advection of wakes past the grid walls deforms the jets into *bean-like shapes* oriented vertically (for stronger jets) or horizontally (for weaker jets). The anisotropic behaviour has two different limits: (i) the one direction is dominating, which is called *cigar* [18], and (ii) two directions are significantly larger than the third one, which is called *pancake* [19]. The actual state of (an)isotropy is displayed in the *Anisotropy invariant map* with axes of the combination of −II and III. As Lumley proved [15], all cases have to lie within the Lumley triangle depicted in panel (d) by grey curves. Here two clouds of all points from both datasets are plotted together with selected points located in the jet between vortices (□ and ◇) and in the vortex centre (○ and ▽).

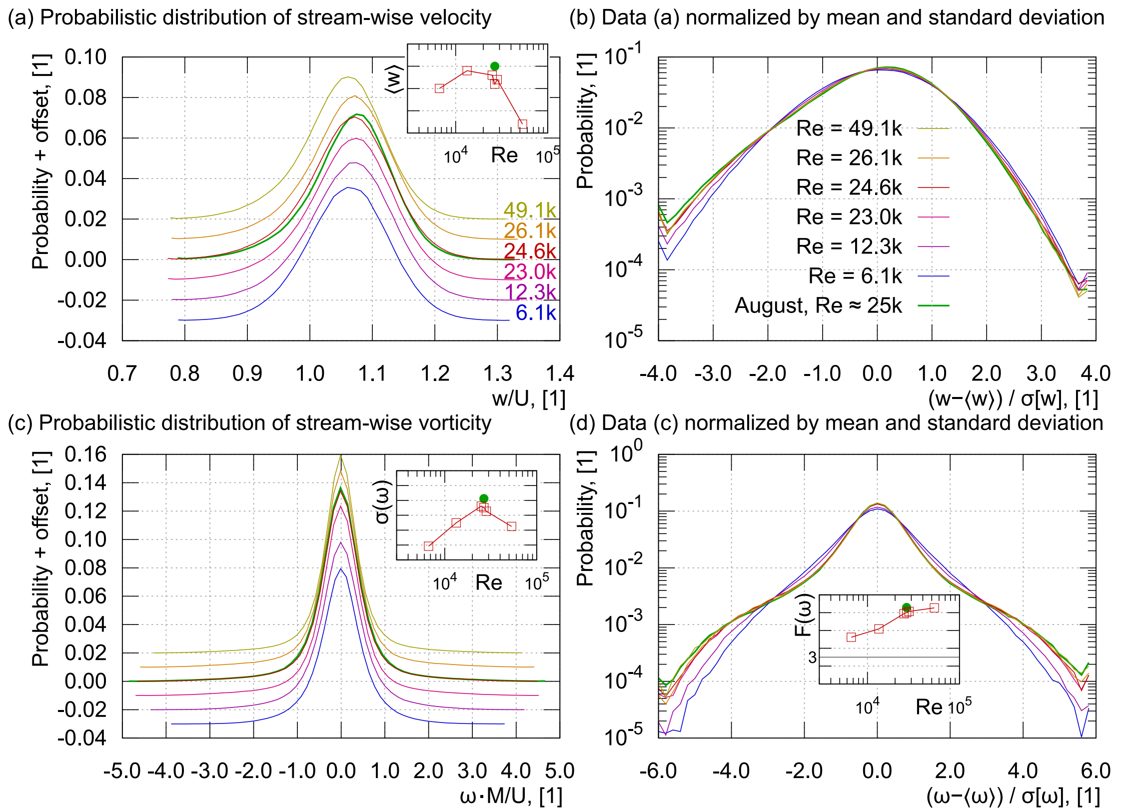

Figure 3: Histograms of the stream-wise velocity (a, b) and stream-wise vorticity (c, d). Left graph display the relative count of a value, while the right-hand plots normalize the x-axis by mean and standard deviation, therefore fine details on the distribution shape can be observed. In the legend, "k" stands for "$\cdot 10^3$", data from August are plotted as green line, other data are measured in October; the Reynolds number is controlled via wind tunnel velocity U. The insert in panel (a) displays he qualitative change of the mean stream-wise velocity $\langle w \rangle$ as a function of Reynolds number. the insert in panel (c) shows the qualitative change of standard deviation of vorticity $\sigma[\omega]$ with Reynolds number and the insert in panel (d) shows the vorticity flatness $F[\omega] = \left\langle (\omega - \langle\omega\rangle)^4 \right\rangle / \sigma^4[\omega]$ with "neutral" value of Gaussian distribution denoted by black line.

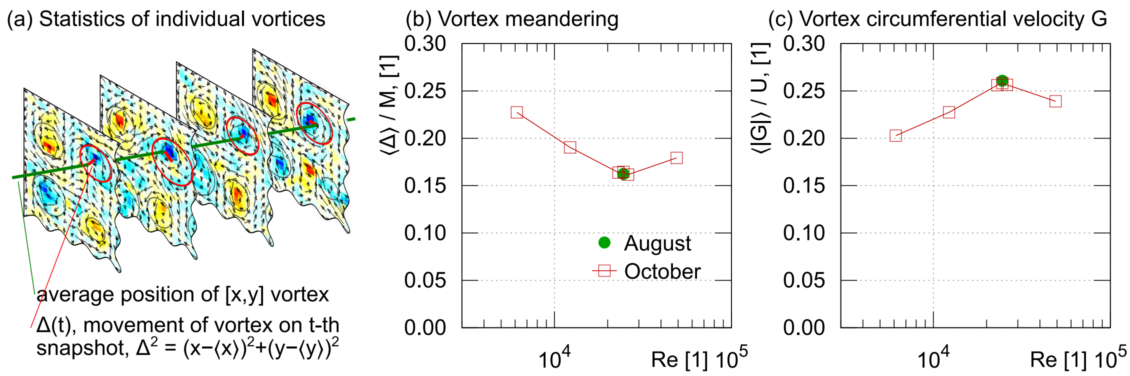

Figure 4: Meandering of vortices around their average positions. Panel (a) schematically shows the deviation $\Delta(t)$ of each vortex at instantaneous time t, panel (b) displays the average value of Δ as a function of Reynolds number. Panel (c) displays the average circumferential velocities G, where $G = \Gamma/(2\pi R)$, Γ vortex circulation and R radius of its core, see [20] for more details.

in the vortex centre, which, according to our opinion, is an artefact of their methodology, when the entire instantaneous velocity field has been rescaled and shifted according to the vortex. The irregularities of the vortex lattice seem to be reproducible: note e.g. the fourth vortex from left in the top line in Figure 1de – it has stronger T_{KE} signal in both realizations. This also suggests, that the differences between August and October has not origin in the uncertainty of grid placement inside the wind tunnel.

Vorticity maps (Fig. 1gh) show the arrangement of antiparallel vortices via their colour. Vorticity is calculated by using spatial gradient only in the measured plane and therefore, it is much more sensitive to noise than just the velocity. To approximate gradient from the discrete grid of data, the second order central differentiation scheme is used. The consequence of this scheme is the impossibility of calculating vorticity near the boundary of FoV, which disturbs even more the plots of higher statistical moments: Fig. 1ij for the standard deviation and Fig. 1lm for the skewness (third statistical moment).

The vorticity standard deviation (Fig. 1ij) displays the same topology like the plot of T_{KE} with maxima at the *average* vortex centres. There is more emerging the tendency of pairing some vortices, e.g. in the top line the first with the second and the third with the fourth.

The vorticity skewness ($A[\omega]$, Fig.1lm) represents the asymmetry of the local distribution: the positive value signifies, that there is smaller amount of stronger events balanced by larger amount of weaker events. Here, one can observe a ring of extrema around the equilibria. This effect is caused by the meandering of instantaneous vortices with expected vorticity maximal in the core, while its decrease in envelope is slow. Very roughly speaking, the radii of those rings can be interpreted as direct evidence of effective meandering amplitude. Fortunately, we have a better method to get this value – the instantaneous vortex fitting [22, 20]. Note that higher statistical moment combined with derivative is very sensitive to noise and thus the structures observable in the spatial maps of $A[\omega]$ are not directly comparable between two cases. But, anyway, the main feature (rings) is reproducible in a qualitative manner as well as the discrepancies between different cells of swirler grid.

3.1 The effect of Reynolds number

According to Reynolds observation [2], the only important parameter next to the geometry is the combination of geometry scale, velocity and viscosity. Viscosity ν is rather complex quantity [23, 24], which depends on density ρ, temperature T and amount of impurities, in the case of air mainly the water represented as the relative humidity $\phi = p_w/p_s(T)$, where p_w is the partial pressure of water vapour and $p_s(T)$ is the saturated pressure at given temperature T. At the laboratory conditions of $p = 9.66 \cdot 10^4\,\mathrm{Pa}$, temperature $T = 298\,\mathrm{K}$ and relative humidity $\phi = 0.42$ the kinematic viscosity can be estimated to $\nu = 1.63 \cdot 10^{-5}\,\mathrm{m^2/s}$. The partial sensitivities near the probed point are

$$\frac{\partial \nu}{\partial p} = -1.7 \cdot 10^{-10}\,\frac{\mathrm{m^2/s}}{\mathrm{Pa}}, \quad \frac{\partial \nu}{\partial T} = 9.4 \cdot 10^{-8}\,\frac{\mathrm{m^2/s}}{\mathrm{K}}, \quad \frac{\partial \nu}{\partial \phi} = -1.1 \cdot 10^{-7}\,\mathrm{m^2/s}. \tag{3}$$

The corresponding partial sensitivities of Reynolds number at working conditions ($M = 25\,\mathrm{mm}, U = 16\,\mathrm{m/s}, p = 96622\,\mathrm{Pa}, T = 298\,\mathrm{K}, \phi = 0.42$) are

$$\frac{\partial \mathrm{Re}}{\partial p} = 0.26\,\mathrm{Pa}^{-1}, \quad \frac{\partial \mathrm{Re}}{\partial T} = -141\,\mathrm{K}^{-1}, \quad \frac{\partial \mathrm{Re}}{\partial \phi} = 166, \quad \frac{\partial \mathrm{Re}}{\partial U} = 1534\,(\mathrm{m/s})^{-1}, \quad \frac{\partial \mathrm{Re}}{\partial M} = 982\,(\mathrm{mm})^{-1}, \tag{4}$$

thus, e.g. the increase of T by $10\,\mathrm{K}$ can be roughly compensated by decrease of U by $1\,\mathrm{m/s}$.

In order to check the possible influence of this, we performed the experiment at different velocities, i.e. different Reynolds numbers. Figure 3 compares the distribution of instantaneous velocities and vorticities; the statical ensemble is taken over all snapshots and over all spatial points measured. The distributions of stream-wise velocity w do not display some qualitative dependence on Reynolds number; the horizontal shift of the values is plotted in the insert of panel (a) of Fig. 3. To compare the *shape*, the distribution is normalized by mean and standard deviation and plotted in logarithmic scale, as it is usual in statistical studies [25, 26].

The vorticity PDF (probability density function) displays straighter polynomial decrease for lower Reynolds numbers, while at larger ones, the distribution is first steeper followed by a bump in the distance of around $4 \times \sigma$. This issue can be the viscosity effect: at larger velocities, the smaller vortices created by turbulent non-linear interactions of the dominating vortex lattice are ejected around the main vortices and they are less damped than at lower velocities, which leads to the observed bumps. The increasing influence of turbulence effects on vortex damping affects the vortex statistics as well: Fig. 4 shows the vortex meandering and circumferential velocity as a function of Re. First, at lower Re, the vortices meander less and are faster with increasing Re as the relative importance of molecular damping decreases. But, when the turbulent damping takes over, then this trend opposes.

4 Conclusions

Interruption of measurement series can lead to emergent doubts about repeatability, which is a key feature of a good scientific experiment. This happened in our laboratory, when we needed to continue some measurement series few months later under different atmospheric conditions (hot dry summer vs. rainy autumn). Therefore we decided to test such influence directly just by repeating one of the last measurement point.

The placement of each instruments lead to the change of *scale of FoV* obtained by calibration by around $8.9 \cdot 10^{-3}$.

The imperfections in geometry caused e.g. by thermal dilatation or by aging of tested geometry seems not to play a role, as the features associated with such kind of imperfections (mainly the loss of symmetry of ensemble-averaged vortices in Fig. 1) are reproducible.

The effect of different Reynolds number caused by different air viscosity is expected to be small. The test of changed Re by changing U displays *repeatable qualitative results, but not quantitative*, see Figs. 3 and 4.

Acknowledgment

The financial support for the present project was partly provided by the *university of West Bohemia* under internal project *SGS-2022-023*.

References

[1] Slezak, P. & Waczulikova, I.: Reproducibility and repeatability. *Physiol Res*, vol. 60 (2011) pp. 203–205.

[2] Reynolds, O.: An experimental investigation of the circumstances which determine whether the motion of water shall be direct or sinuous, and of the law of resistance in parallel channels. *Philosophical Transactions of the Royal Society of London*, vol. 174 (1883) pp. 935–982.

[3] Strouhal, V.: Ueber eine besondere art der tonerregung. *Annalen der Physik*, vol. 241 (1878) pp. 216–251.

[4] Keulegan, G. & Carpenter, L.: Forces on cylinders and plates in an oscillating fluid. *J. Res. Nat. Inst. Stand.*, vol. 60 (1958) pp. 423–440.

[5] Králík, T., Musilová, V. & Skrbek, L.: Modulated turbulent convection: a benchmark model for large scale natural flows driven by diurnal heating. *Scientific Reports*, vol. 14 no. 1: (2024).

[6] Skrbek, L., Niemela, J. J. & Urban, P.: Utilization of cryogenic phases of helium as ?magic? working fluids in laboratory experiments: Pushing the boundaries of fluid dynamics. *Physics of Fluids*, vol. 36 no. 10: (2024).

[7] Yanovych, V., Tsymbalyuk, V. & Uruba, V.: Effect of manufacturing inaccuracies on the wake past asymmetric airfoil by piv. *Energies*, vol. 15 (2022) p. 1227.

[8] Duda, D., Tomášková, T. & Uruba, V.: Hot-wire investigation of turbulence topology behind blades at different shape qualities. *Processes*, vol. 10 (2022) p. 522.

[9] Duda, D.: How manufacturing inaccuracies affect vortices in an airfoil wake. in *Proceedings Topical Problems of Fluid Mechanics 2021* (Šimurda, D. & Bodnár, T., eds.) pp. 48–55 (2021).

[10] Duda, D. & Yanovych, V.: Interaction of stream-wise vortices generated by swirler grid. *Physics of Fluids*, vol. 36 no. 5: (2024).

[11] Tropea, C., Yarin, A. & Foss, J. F.: *Springer Handbook of Experimental Fluid Mechanics.* Springer, Heidelberg, DE (2007).

[12] Duda, D., Horáček, V. & Uruba, V.: Research of a wind tunnel parameters by means of cross-section analysis of air flow profiles. *AIP Conference Proceedings*, vol. 2189 no. 020024: (2019).

[13] Vignat, G., Durox, D. & Candel, S.: The suitability of different swirl number definitions for describing swirl flows: Accurate, common and (over-) simplified formulations. *Progress in Energy and Combustion Science*, vol. 89 (2022) p. 100969.

[14] Bennett, S.: A brief history of automatic control. *IEEE Control Systems Magazine*, vol. 16 no. 3: (1996) pp. 17–25.

[15] Lumley, J. & Newman, G.: The return to isotropy of homogeneous turbulence. *J. Fluid Meach.*, vol. 82 (1977) pp. 161–178.

[16] Hamilton, W. R.: On the existence of a symbolic and biquadratic equation which is satisfied by the symbol of linear or distributive operation on a quaternion. *The London, Edinburgh, and Dublin Philosophical Magazine and Journal of Science*, vol. 24 (1862) pp. 127 – 128.

[17] Motl, L. & Zahradník, M.: *Pěstujeme lineární algebru.* Matfyzpress (1994).

[18] Choi, K. & Lumley, J.: The return to isotropy of homogeneous turbulence. *J. Fluid Meach.*, vol. 436 (2001) pp. 59–84.

[19] Simonsen, A. & Krogstad, P.: Turbulent stress invariant analysis: Clarification of existing terminology. *Phys. Fluids*, vol. 17 (2005) p. 088103.

[20] Duda, D.: Searching of individual vortices in experimental data. in *Vortex Dynamics – From Physical to Mathematical Aspects [Working Title]* (Bakırtaş, I. & Antar, N., eds.) IntechOpen (2021).

[21] Ben Miloud, K., Ferchichi, M. & Fellouah, H.: Meandering of a wing-tip vortex in a grid-generated turbulent flow. *Physics of Fluids*, vol. 33 no. 11: (2021).

[22] Duda, D.: Individual vortex searching algorithm. in *In Proceedings Topical Problems of Fluid Mechanics 2020* (Šimurda, D. & Bodnár, T., eds.) pp. 56–63 (2020).

[23] Kestin, J. & Whitelaw, J.: The viscosity of dry and humid air. *International Journal of Heat and Mass Transfer*, vol. 7 no. 11: (1964) pp. 1245–1255.

[24] Buddenberg, J. W. & Wilke, C. R.: Calculation of gas mixture viscosities.. *Industrial and Engineering Chemistry*, vol. 41 no. 7: (1949) pp. 1345–1347.

[25] Belin, F., Maurer, J. & Willaime, H.: Probability density functions, skewness, and flatness in large reynolds number turbulence. *PHYSICAL REVIEW E*, vol. 53 (1996) pp. 1613–1621.

[26] Švančara, P., Duda, D. & Skrbek, L.: Small-scale universality of particle dynamics in quantum turbulence. *Physical Review B*, vol. 94 no. 18: (2016).